Directional Adhesive Structures for Controlled Climbing on Smooth Vertical Surfaces

Daniel Santos, Sangbae Kim, Matthew Spenko, Aaron Parness, Mark Cutkosky
Center for Design Research
Stanford University
Stanford, CA 94305-2232, USA
contact: dsantos@stanford.edu

***Abstract*— Recent biological research suggests that reliable, agile climbing on smooth vertical and overhanging surfaces requires controllable adhesion. In nature, geckos control adhesion by properly loading the compliant adhesive structures on their toes. These strongly anisotropic dry adhesive structures produce large frictional and adhesive forces when subjected to certain force/motion trajectories. Smooth detachment is obtained by simply reversing these trajectories. Each toe's hierarchical structure facilitates intimate conformation to the climbing surface resulting in a balanced stress distribution across the entire adhesive contact area. By controlling the internal forces among feet, the gecko can achieve the loading conditions necessary to generate the desired amount of adhesion. The same principles have been applied to the design and manufacture of feet for a climbing robot. The manufacturing process of these Directional Polymer Stalks is detailed along with test results comparing them to conventional adhesives.**

I. Introduction

As mobile robots extend their range of traversable terrain, there has been an increasing interest in mobility on vertical surfaces. Previous methods of climbing include using suction [16], [17], [32], magnets [6], [28], and a vortex [27] to adhere to a variety of smooth, flat, vertical surfaces. Although there has been some success using these solutions (notably [27]) on non-smooth surfaces, in general, the variety of climbable surfaces is limited. In addition, these methods all consume significant energy to create adhesive forces. Taking cues from climbing insects, researchers have designed robots that employ large numbers of small ($10-15\mu$m tip radius) spines that cling to surface asperities [1], [21]. This approach works well for outdoor building surfaces such as concrete or brick but cannot be used for smooth surfaces like glass.

Recently, a number of robots have been demonstrated that use adhesive materials for climbing. Early approaches used pressure-sensitive adhesives (PSAs) to climb smooth surfaces [9], [18], [25], while more recent approaches have used elastomeric pads [3], [8], [26]. PSAs tend to foul quickly, which prevents repeated use, and also require relatively high energy for attachment and detachment. Elastomer pads are less prone to fouling, but generate lower levels of adhesion.

In an effort to create an adhesive that does not become fouled over time, there has been research on "dry" or "self-cleaning" adhesives that utilize stiff materials in combination with microstructured geometries to conform to surfaces.

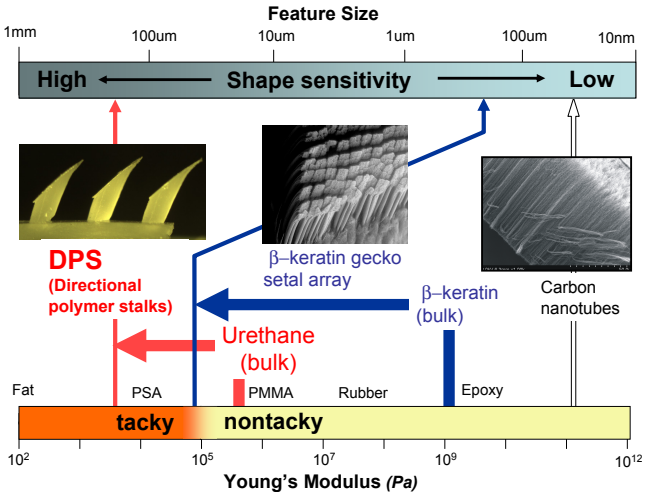

Fig. 1. Shape sensitivity of different structures and modulus of elasticity of various materials. Microstructured geometries can lower the overall stiffness of bulk materials so that they become tacky. This principle allows geckos to use β-keratin for their adhesive structures and can be applied to other materials as well.

Figure I shows the range of adhesive solutions ordered in terms of feature size and effective modulus. A material is considered tacky when the effective modulus is less than 100kPa [2], [7]. All of the solutions adhere primarily as a result of van der Waals forces, which decrease as $1/d^3$ where d is the distance between the two materials. Consequently, it is crucial to conform to the surface as well as possible over all relevant length scales. PSAs achieve this conformation by yielding and flowing when subjected to pressure.

Dry adhesives, such as the gecko hierarchy of microstructures consisting of lamellae, setae and spatulae, achieve similar conformabilities despite having bulk material stiffnesses that are relatively high (approximately 2GPa for β-keratin) [2]. The hieirarchical geometry of the gecko dry adhesive lowers the effective stiffness enough to make the system function like a tacky material.

Synthetic dry adhesives have been under development for several years. Examples include arrays of vertically oriented multiwall carbon nanotubes [30], [31] and vertically oriented arrays of polymer fibers [11], [14], [19], [24]. These examples employ stiff, hydrophobic materials and therefore

have the potential to become self-cleaning at small scales, like the gecko setae. In a number of cases, useful levels of adhesion have been obtained, but only with careful surface preparation and high preloads. As the performance of these synthetic arrays improves, their effective stiffnesses could approach the "tack criterion" seen in the gecko.

A different approach is to use structured arrays of moderately soft elastomeric materials with a bulk stiffness on the order of $300\mathrm{kPa}$. Because these materials are softer to begin with, they conform to surfaces using feature sizes on the order of $100\mu\mathrm{m}$ instead of $1\mu\mathrm{m}$ or less needed for stiffer materials. One example is a microstructured elastomeric tape [8], [20]. Because the material is not very stiff, it attracts dirt. However, in contrast to PSAs, it can be cleaned and reused. The microstructured adhesive patches that we describe in Section III, termed Directional Polymer Stalks (DPS) (see Figure I), also employ an elastomer, but are designed to exhibit adhesion only when loaded in a particular direction during climbing.

In addition to the stiffness of a material, the feature size and shape of the structure is also important in determining overall adhesion. As discussed in [10], [29], the available adhesive force is a function of the shape and loading of the micro-structured elements. It is more important for large contacting features than for small ones to optimize the tip shape and avoid contact stress concentrations that lead to crack formation and peeling. For extremely small elements such as carbon nanotubes, the distal geometry is relatively unimportant, but for features on the order of hundreds of $\mu\mathrm{m}$, tip geometry can drastically affect adhesion. At these sizes, the optimal tip geometry, where stress is uniformly distributed along the contact area, has a theoretical pulloff force of more than 50-100 times [10] that of a poor tip geometry, where cracks immediately initiate due to stress concentrations. In general, larger features must be designed with more optimal tip shapes in order to achieve tackiness. In Section III we describe the processes we have developed to obtain desired shapes at the smallest sizes our current manufacturing procedures allow and in Section IV we present experimental results obtained with these shapes.

II. Anisotropic versus isotropic adhesion

At present, no synthetic solution has replicated the adhesion and self-cleaning properties of gecko feet. However, as we argue in the following sections, the main obstacle to robust climbing is not *more* adhesion but *controllable* adhesion. Sticky tape is sufficiently adhesive for a lightweight climbing robot, but its adhesive forces are difficult to control. Geckos control their adhesion with *anisotropic* microstructures, consisting of arrays of setal stalks with spatular tips. Instead of applying high normal preloads, geckos increase their maximum adhesion by increasing shear load, pulling from the distal toward the proximal ends of their toes. In conjunction with their hieirarchical hairy structures, this provides geckos with a coefficient of adhesion, $\mu' = F_a/F_p$, between 8 and 16 depending on conditions, where F_a is the maximum pulloff force and F_p is the maximum normal preload [2].

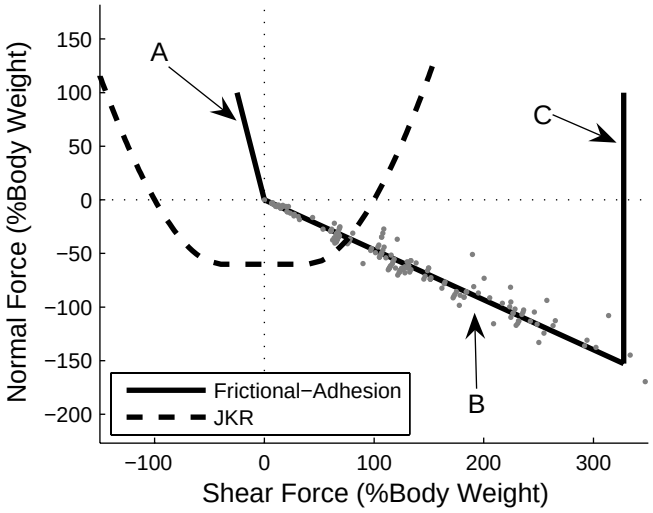

Fig. 2. Comparison of frictional-adesion and JKR contact models. Both models have been scaled to allow a 50g gecko or robot to cling to an inverted surface. The anisotropic frictional-adhesion model is based on parameters in [3]. Data overlayed on the frictional-adhesion model is from [3], [5] for gecko setae, setal arrays, and toes. The isotropic JKR model is based on parameters in [20], [22].

A. Description of Contact Models

A frictional-adhesion model (Figure 2) is used as a simple way to describe the gecko adhesion system [3]. When pulling along the adhesive direction (B), the maximum adhesive force is directly proportional to the applied shear force:

$$-F_N \leq F_T \tan \alpha^* \tag{1}$$

where F_N is the adhesive force, F_T is the tangential force (positive when pulling from distal to proximal), and α^* is the angle of a best fit line for test data obtained with individual setae, setal arrays, and gecko toes [3]. When pulling against the adhesive direction (A), the behavior is described by the Coulomb friction law. An upper limit is placed on the maximum shear in the adhesive direction (C), which will be a function of limb and material strength.

Figure 2 compares frictional-adhesion and the Johnson-Kendall-Roberts (JKR) model [12], an isotropic adhesion model based on a spherical elastic asperity in contact with a flat substrate. This model predicts that maximum adhesion occurs in the absence of any shear loads. Increasing shear load decreases the contact area, thereby decreasing the overall adhesion. For positive values of normal force $F_T \propto {F_N}^{2/3}$ [23]. The models have been scaled to give comparable values of adhesion and shear limits and the curves represent the maximum values of normal and tangential force at which a contact will either slide or pull apart.

The anisotropic model shows how maximum adhesion can be controlled simply by decreasing the shear load at the contact. Its intersection with the origin allows for contact termination with negligible forces, whereas the isotropic model, which does not intersect the origin, predicts large force discontinuities at contact termination. The anisotropic model would also be better-suited for vertical climbing than the isotropic. If the anisotropy is aligned properly, then gravity could passivly load the contact in a way that increases

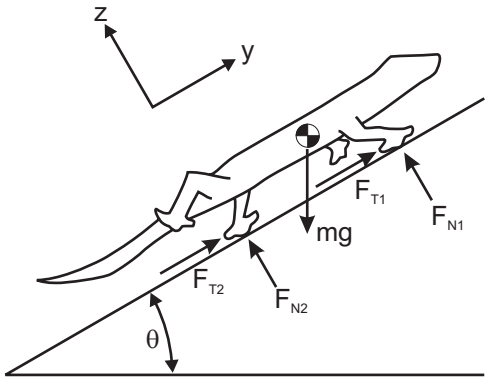

Fig. 3. 2-Dimensional model of gecko with two feet in contact with a flat inclined plane. Foot-substrate interactions are assumed to be point contacts with two forces acting at the contact. Gravity acts on the center of mass of the system.

adhesion, whereas for the isotropic model, gravity could only decrease adhesion on vertical surfaces as it would increase shear loads.

B. Implications for control of contact forces

In general, both anisotropic and isotropic adhesives may provide adhesion comparable to the body weight of a gecko or a robot; however, the anisotropic and isotropic models lead to different approaches for controlling contact forces during climbing. A simplified planar model of a climbing gecko or robot (Figure 3) is useful for studying the implications of different contact models. Work in dexterous manipulation [13] is adapted to study the static stability of the model on inclined surfaces. There are four unknowns and three equilibrium constraints, leaving one degree of freedom: the balance of shear load between the front and rear foot (i.e. the internal force), $F_{Int} = F_{T1} - F_{T2}$. In turn, the shear load that each foot can withstand is limited by the contact model used for the foot-substrate interaction.

The stability of the system can be used to determine how best to distribute contact forces between the feet. The stability margin is the minimum distance, in force-space, over all feet, that any given foot is from violating the contact constraints. It defines the maximum perturbation force that the system can withstand without failure of any foot contacts.

Let $\mathbf{F_i} = [F_{Ti}, F_{Ni}]$ be the contact force at the i^{th} foot. The contact model can be defined by a parametric convex curve $\mathbf{R}(x, y)$, with points $\mathbf{F} = [F_T, F_N]$ lying inside the curve being stable contacts. The distance any particular foot is from violating a contact constraint is then

$$d_i = \min_{x,y}(||\mathbf{F_i} - \mathbf{R}(x, y)||) \tag{2}$$

For a model with two feet in contact with the surface, the overall stability margin becomes $d = \min(d_1, d_2)$, where d_1 is the front foot and d_2 is the rear foot.

The 2-D model's extra degree of freedom (the internal force) can be used to maximize the stability margin. This produces very different force control strategies using the anisotropic or isotropic models at different surface inclines (Figure 4). On a vertical surface the front foot contact must generate adhesion for stability. The anisotropic model predicts that the front foot should bear more shear load, since increasing shear load in the adhesive direction increases maximum available adhesion. The isotropic model predicts the opposite, namely that the rear foot should bear more shear load, because shear loads on the front foot decrease its available adhesion. On a fully inverted surface, the isotropic model predicts zero shear loads for stability since gravity is pulling along the normal, purely adhesive direction. Alternatively, the anisotropic model cannot generate adhesion without shear loads and so it predicts that the model must rotate the rear foot and pull inward with both feet in order to generate the shear loads that will produce enough adhesion for stability. Interestingly, the anisotropic model predicts that reversing the rear foot and pulling inward is also optimal on level ground. While stability may not be critical on level ground, this would indeed increase the maximum perturbation force (i.e. gusts of wind) that could be withstood. The predictions of the anisotropic model qualitatively match observations of geckos running up vertical surfaces and reorienting their feet as they climb in different directions [4].

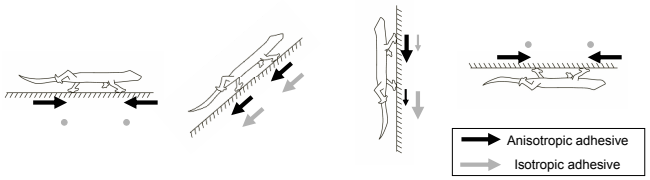

Fig. 4. Schematic of shear forces for isotropic and anisotropic adhesion at different surface inclines. Arrow directions and magnitudes shown in proportion to optimatl shear forces (dot represents zero shear load).

III. Design and Manufacturing of Anisotropic Adhesive Pads

The importance of anisotropic adhesion has been demonstrated on a new experimental robot, Stickybot (Figure 5), which was designed to climb with anisotropic adhesion. Details of the overall design and control of Stickybot are covered in a companion paper [15]. In this section we explain the manufacturing process that allows us to create DPS, and in the next section we present test results analyzing the DPS and comparing them to isotropic stalks of equivalent size and density.

The anisotropic stalks used on the bottom of Stickybot's feet are fabricated from a polyurethane (Innovative Polymers, IE-20 AH Polyurethane) with a Shore-20A hardness and an elastic modulus of about $300\mathrm{kPa}$. Custom miniature tooling was used to create a mold from which the DPS were fabricated (Figure 6). The stalks are cylindrical and tilted with respect to the backing. The upper stalk is cropped at an oblique angle that creates a sharp tip. The cylinders are $380\mu\mathrm{m}$ in diameter and approximately $1.0\mathrm{mm}$ long from base to tip. Empirically, it has been found that best results are obtained with the cylinder axes inclined at $20°$ with respect to the vertical and slanted tips inclined at $45°$ with respect to the vertical. The shape of the stalks is defined

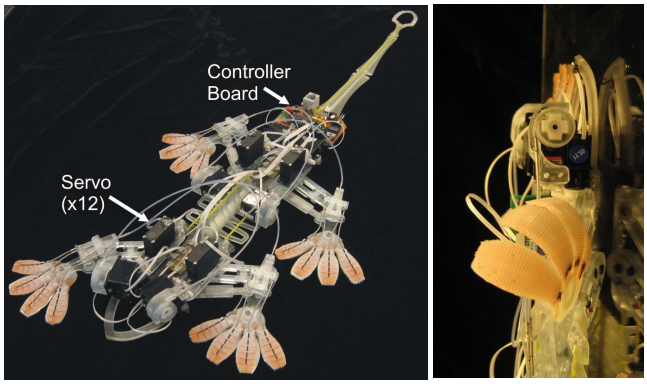

Fig. 5. Stickybot experimental climbing robot for testing directional adhesives. Each limb has two trajectory degrees of freedom (fore-aft and in-out of the wall) and one toe-peeling degree of freedom. The entire robot weighs 370 grams.

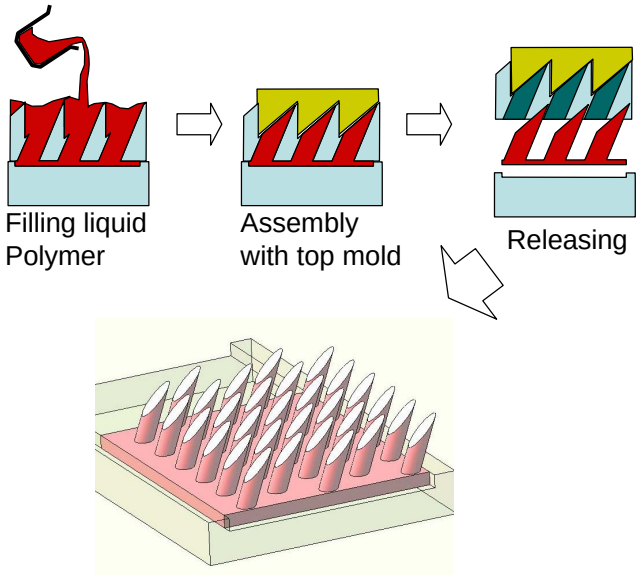

Fig. 6. Molding process used to fabricate aniostropic patches. Mold is manufactured out of hard wax and then filled with liquid urethane polymer. Cap eliminates contact with air and creates final tip geometry.

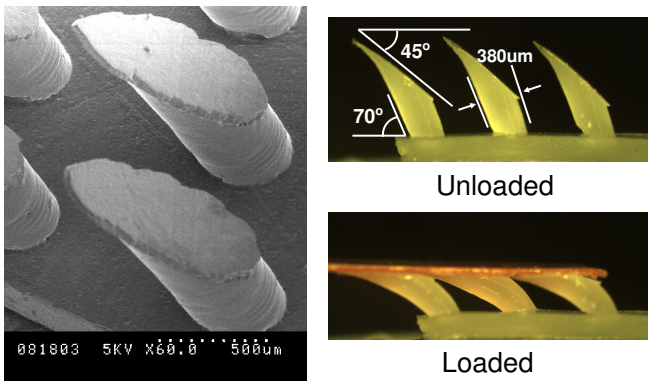

Fig. 7. SEM Picture of anisotropic stalks. Stalks are oriented at 70° with respect to normal and stalk faces are oriented at 45° with respect to normal. Stalk diameter is 380μm.

by the intersections of slanted circular holes with narrow Vee-shaped grooves. First, the grooves are cut into the mold using a custom 45° degree slitting saw. This angle dictates the angle of the tip with respect to vertical. Next, slanted circular holes are drilled into the grooves at a 20° such that the opening resides entirely on the 45° face of the groove.

To create the DPS, liquid polymer is poured into the mold and capillary action fills the holes. Attempts were first made to wipe excess polymer out of the grooves and allow the urethane to cure exposed to atmosphere. This can lead to softer, stickier tips but is difficult to control and can cause the final cured urethane to degrade with time. To overcome these limitations, a silicone (TAP Plastics, Silicone RTV Fast Cure Mold-Making Compound) form-fitting cap is molded from the Vee grooves before holes are created. The form-fitting cap is then pressed down into the grooves, forcing excess polymer out the sides and eliminating the need for a wiping step (Figure 6. In this case, the urethane cures uniformly and the manufacturing repeatability is superior than when not using the cap. Furthermore, the stalks molded with the form-fitting cap have greatly increased durability and, when dirty, recover performance almost fully after cleaning. An SEM photo of the stalks created using this molding process is shown in Figure 7.

The DPS manufactured by these processes narrow to a sharp, thin tip ($10 - 30\mu$m thickness). When the stalks are first brought into contact with a surface, this tip adheres and the amount of shear force required to engage the remaining area of the DPS face is very low. Figure 7 shows the geometry of the stalks in both the unloaded and loaded states.

IV. Adhesion Tests and Results

Specimens of the anisotropic material described in the previous section were tested under a variety of shear and normal loading conditions to characterize their adhesive properties. For comparison, an array of isotropic cylinders (vertical cylinders of the same diameter with flat tops) made from the same polymer was also tested.

Both the anisotropic and isotropic patches were approximately elliptical with a total area of $3.5 - 4\text{cm}^2$, corresponding to one toe of Stickybot, which has four such toes per foot. Within that area, anisotropic specimens contained about 500 individual stalks while isotropic specimens contained about 250 stalks. The total area of oblique upper faces in the anisotropic specimens was approximately 1.38cm^2 and of cylinder tops in the isotropic specimen approximately 0.29cm^2. These values represent upper bounds for the maximum contact area. Specimens were prepared by washing them in tap water and then blowing dry with compressed air. They were mounted using thin double-sided tape to a flat aluminum backing.

The specimens and aluminum backing were fixed on a two-axis linear positioning stage (Velmex MAXY4009W2-S4) driven under servo control at 1kHz. The specimens were brought into contact with a stationary glass plate affixed to a 6-axis force/torque measurement device (ATI Gamma Transducer). The positioning stage is a stiff, screw driven

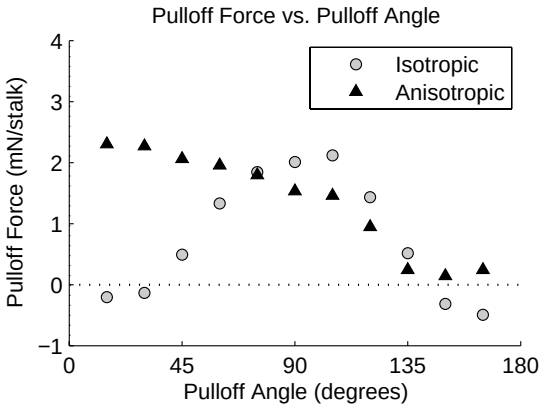

Fig. 8. Adhesion forces as a function of pulloff angle for anisotropic and isotropic patches. For anisotropic patches, maximum adhesion is attained when the pulloff angle is shallow and in the adhesive direction. Adhesion drops steadily as the angle becomes normal to the surface and becomes negligible at shallow angles in the non-adhesive direction. For isotropic patches, maximum adhesion is attained when pulling off normal to the surface and drops rapidly at angles on either side of the normal.

device and achieves a trajectory accuracy of approximately $+/-20\mu\mathrm{m}$ while in motion at speeds of $1\mathrm{mm/s}$. The resolution of the 6-axis sensor is approximately $25\mathrm{mN}$ and $0.5\mathrm{mNm}$ for forces and torques, respectively. Force and torque data were sampled at $1\mathrm{kHz}$ and filtered at $10\mathrm{Hz}$ using a $3^{\mathrm{rd}}-\mathrm{order}$ Butterworth filter.

Following a procedure used to measure gecko setal array adhesion forces [3], the synthetic patches were moved along a controlled trajectory in the normal and tangential directions while measuring the resulting forces. Specimens were brought into contact with the glass substrate and then preloaded to a specified depth in the normal axis. The approach angle for the anisotropic patches was set to 45°, moving with the stalk angle (i.e. loading the stalks in the preferred direction for adhesion), and for the isotropic patch along the normal direction (90°). The patches were then pulled away from the glass substrate at departure angles between 15° (mostly parallel to the surface, with the angle of the anisotropic stalks) and 165° (mostly parallel to the surface, against the angle of the anisotropic stalks). In all cases, velocity was maintained at $1\mathrm{mm/s}$, which was determined empirically to provide a favorable tradeoff between avoiding dynamic forces while also minimizing any effects of viscoelastic creep.

Figure 8 illustrates the performance of the stalks as a function of pulloff angle. In general, the anisotropic patches produce maximum values of adhesion when loaded primarily in shear, as a robot would load them when clinging to a vertical wall. At angles less than 30°, the maximum adhesion force is approximately $2.3\mathrm{mN/stalk}$ (1.2N for the entire patch), and the corresponding value of μ' was approximately 4.5. Pulling off in the normal direction generates adhesion of about $2/3$ the peak value and when pulling off against the angle of the stalks the adhesion drops to less than 10% the peak value. For the isotropic patch, maximum adhesion is obtained when pulling off in the purely normal direction, dropping to zero for pulloff angles slightly over 45° with respect to the normal. The isotropic patch has a maximum adhesive force nearly as high as the anisotropic patches, but requires a higher preload, resulting in a μ' of approximately 0.5.

Figure 9 summarizes the results for the maximum tangential and normal forces of the different patches at pulloff over a range of preload depths and pulloff angles. The results can be compared directly with the models in Figure 2. As expected, the isotropic specimen shows a behavior similar to that predicted by the JKR model: The limit curve is symmetric about the vertical axis, meaning that there is no preferred direction for adhesion. Maximum adhesion is obtained when pulling in the purely normal direction, and under positive normal load Coulomb friction is observed.

The anisotropic patches exhibit a behavior similar to that of the gecko setae. Fitting a line to the data for positive values of tangential force results in an estimate of $\alpha^* \approx 20^\circ$ (compared to approximately 30° for the gecko [3]). When loaded against their preferred direction ($F_t < 0$) they exhibit a moderate coefficient of friction, and, between these two modes, the data intersects the origin. Thus, like the gecko setae, the synthetic patches can easily be detached by controlling internal forces so as to reduce the tangential load. However, unlike the gecko setae, the synthetic stalks start to lose adhesion at high levels of shear force, at which point the contact faces of the stalks start to slip. This can be seen in the saturation of the maximum adhesion force.

Figure 9 also shows that the data for isotropic and anisotropic patches scales with increasing preload. For the isotropic patches, maximum adhesion is obtained when the specimen is preloaded to approximately $300\mu\mathrm{m}$ after initial contact, resulting in a normal preload of about $14.3\mathrm{mN/stalk}$. For the anistropic patches, a $700\mu\mathrm{m}$ preload depth provided maximum adhesion, which corresponds to about $0.5\mathrm{mN/stalk}$. Larger preloads resulted in no further significant increase in adhesion; smaller preloads produced less adhesion, indicated by those symbols that lie inside the outermost limit curves.

Given the foregoing results, anisotropic and isotropic specimens can be expected to produce rather different effects when used on a robot. Figure 10 shows typical force plots for anisotropic and isotropic toe patches on the Stickybot robot. The data for three successive cycles are plotted to show overall variability. In each case, the robot cycled a single leg through an attach/load/detach cycle on the same 6-axis force sensor in the previous tests now mounted into a vertical wall. The other three limbs remained attached to the wall throughout the experiment. In this test, the isotropic patches consisted of vertical cylinders with a thin upper membrane bridging the gaps between the cylinders. This was done to increase the contact area, otherwise the isotropic patch required too much preload for the robot to climb on vertical surfaces. The leg has two degrees of freedom allowing independent motion in the fore-aft direction and in the direction into and out of the wall. In addition, the toes of Stickybot have an active peeling and flexing mechanism that facilitates detachment at the end of stroke [15]. In each case, the two leg axes and the flexing/peeling servo were

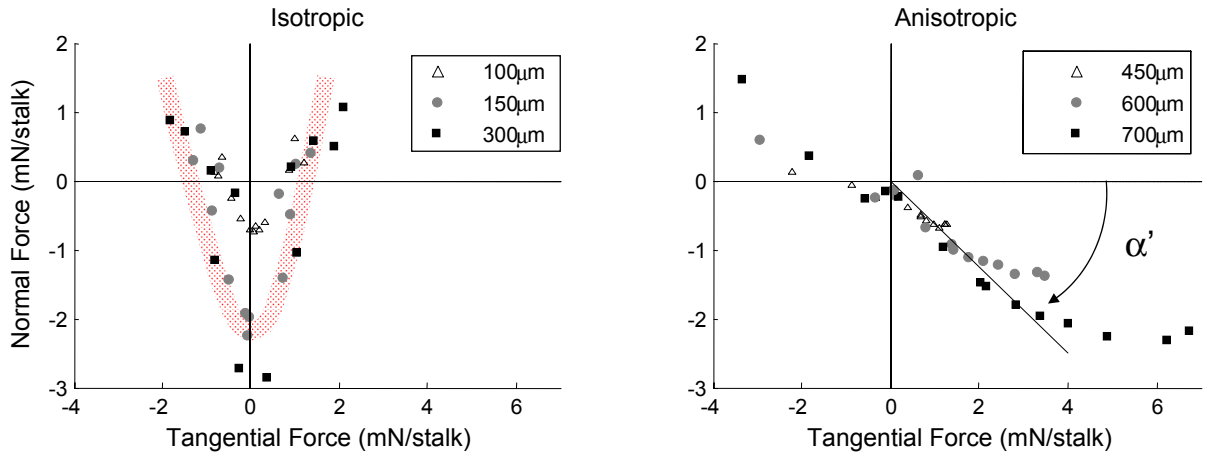

Fig. 9. Experimental limit curves for isotropic and anisotropic patches at different preload depths. Data points correspond to maximum forces at pulloff. Three series have been plotted to show the dependence of limit curves on the preload.

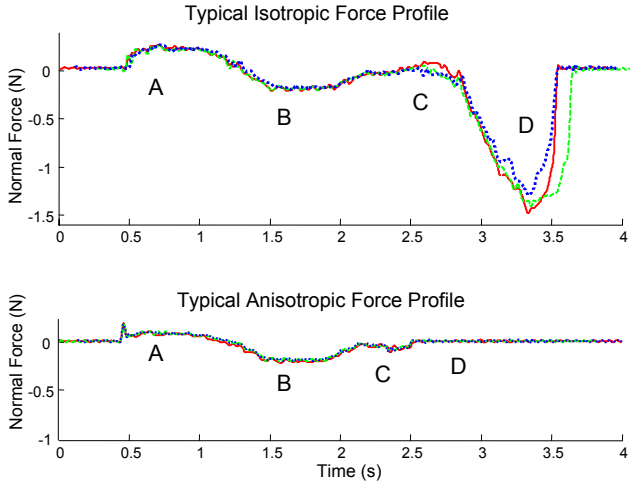

Fig. 10. Comparison of normal force profiles of anisotropic and isotropic patches on a climbing robot. Point A on the curves refers to the preloading phase of the cycle. Point B highlights when the foot is in the adhesive regime during a stroke. Points C and D are when the foot is unloaded and detached, causing large normal forces in the case of the isotropic patch.

tuned empirically to provide best results for the isotropic or anisotropic patches.

As the plots show, the isotropic patches required a somewhat larger normal force (A) to produce comparable amounts of combined shear force and adhesion for climbing (B). The unloading step for the anisotropic patches (C, D) is accomplished rapidly and results in negligible detachment force as the leg is removed. In contrast, the isotropic patch requires a longer peeling phase (C) and produces a very large pulloff force (D) as the leg is withdrawn. This large detachment force was the main limitation of the isotropic patches, producing large disturbances that frequently caused the other feet to slip.

V. Conclusions and Future Work

This paper describes the design and manufacturing method for novel adhesive toes and presents experimental evidence that emphasizes the importance of controllable directional adhesion for a climbing robot. A model of gecko adhesion is presented and compared to a commonly used isotropic model from the literature, the JKR model. It is shown that the anisotropic nature of the frictional-adhesion model, combined with the fact that at zero shear load there is zero adhesive force, allows a robot to smoothly load and unload a foot. Current and future work entails scaling down the size of the anisotropic stalks in order to utilize harder materials and climb rougher surfaces. This will allow for feet that are easier to clean, yet still conform and adhere well to surfaces. It is also important to extend our understanding of anisotropic adhesion to three dimensions and incorporate dynamics into our climbing model. This may better predict and explain the behavior of climbing geckos and guide the design and control of climbing robots.

Acknowledgment

Many thanks to Kellar Autumn and his students for many discussions on anisotropic adhesion and advice on testing procedure. This work was supported through the DARPA BioDynotics Program, the Intelligence Community Postdoctoral Fellow Program, and the Stanford-NIH Biotechnology Training Grant.

References

[1] A. Asbeck, S. Kim, M. Cutkosky, W. Provancher, and M. Lanzetta. Scaling hard vertical surfaces with compliant microspine arrays. *International Journal of Robotics Research*, 2006.

[2] K. Autumn. *Biological Adhesives*, volume XVII. Springer-Verlag, Berlin Heidelberg, 2006.

[3] K. Autumn, A. Dittmore, D. Santos, M. Spenko, and M. Cutkosky. Frictional adhesion: a new angle on gecko attachment. *J Exp Biol*, 209(18):3569–3579, 2006.

[4] K. Autumn, S. T. Hsieh, D. M. Dudek, J. Chen, C. Chitaphan, and R. J. Full. Dynamics of geckos running vertically. *J Exp Biol*, 209(2):260–272, 2006.

[5] K. Autumn, Y. A. Liang, S. T. Hsieh, W. Zesch, W.-P. Chan, W.T. Kenny, R. Fearing, and R.J. Full. Adhesive force of a single gecko foot-hair. *Nature*, 405:681–685, 2000.

[6] C. Balaguer, A. Gimenez, J. Pastor, V. Padron, and C. Abderrahim. A climbing autonomous robot for inspection applications in 3d complex environments. *Robotica*, 18(3):287–297, 2000.

[7] C.A. Dahlquist. Pressure-sensitive adhesives. In R.L. Patrick, editor, *Treatise on Adhesion and Adhesives*, volume 2, pages 219–260. Dekker, New York, 1969.

[8] K. Daltorio, S. Gorb, A. Peressadko, A. Horchler, R. Ritzmann, and R. Quinn. A robot that climbs walls using micro-structured polymer feet. In *International Conference on Climbing and Walking Robots (CLAWAR)*, 2005.

[9] K. Daltorio, A. Horchler, S. Gorb, R. Ritzmann, and R. Quinn. A small wall-walking robot with compliant, adhesive feet. In *International Conference on Intelligent Robots and Systems*, 2005.

[10] H. Gao, X. Wang, H. Yao, S. Gorb, and E. Arzt. Mechanics of hierarchical adhesion structures of geckos. *Mechanics of Materials*, 37:275–285, 2005.

[11] N. Glassmaker, A. Jagota, and C. Y. Hui. Adhesion enhancement in a biomimetic fibrillar interface. *Acta Biomaterialia*, 1:367–375, 2005.

[12] K.L. Johnson, K. Kendall, and A.D. Roberts. Surface energy and the contact of elastic solids. *Proceedings of the Royal Society A: Mathematical, Physical and Engineering Sciences*, 324(1558):301–313, 1971.

[13] J. Kerr and B. Roth. Analysis of multifingered hands. *The International Journal of Robotics Research*, 4(4):3–17, 1986.

[14] D. Kim, H. Lee, J. Lee, S. Kim, K-H Lee, W. Moon, and T. Kwon. Replication of high-aspect-ratio nanopillar array for biomimetic gecko foot-hair prototype by uv nano embossing with anodic aluminum oxide mold. *J Microsystem Technologies*, 2006.

[15] S. Kim, M. Spenko, S. Trujillo, B. Heyneman, V. Matolli, and M. Cutkosky. Whole body adhesion: hierarchical, directinoal and distributed control of adhesive forces for a climbing robot. In *ICRA*, volume ?, page ?, Rome, Italy, 2007. IEEE. Submitted.

[16] G. La Rosa, M. Messina, G. Muscato, and R. Sinatra. A lowcost lightweight climbing robot for the inspection of vertical surfaces. *Mechatronics*, 12(1):71–96, 2002.

[17] R. Lal Tummala, R. Mukherjee, N. Xi, D. Aslam, H. Dulimarta, J. Xiao, M. Minor, and G. Dang. Development of a tracked climbing robot. *Journal of Intelligent and Robotic Systems*, 9(4), 2002.

[18] P. Menzel and F. D'Aluisio. *Robo Sapiens*. MIT Press, 2000.

[19] M. Northen and K. Turner. A batch fabricated biomimetic dry adhesive. *Nanotechnology*, 16:1159–1166, 2005.

[20] A. Peressadko and S.N. Gorb. When less is more: experimental evidence for tenacity enhancement by division of contact area. *Journal of Adhesion*, 80(4):247–261, 2004.

[21] A. Saunders, D. Goldman, R. Full, and M. Buehler. The rise climbing robot: body and leg design. In *SPIE Unmanned Systems Technology VII*, volume 6230, Orlando, FL, 2006.

[22] A.R. Savkoor and G.A.D. Briggs. The effect of tangential force on the contact of elastic solids in adhesion. *Proceedings of the Royal Society A: Mathematical, Physical and Engineering Sciences*, 356(1684):103–114, 1977.

[23] A. Schallamach. The load dependence of rubber friction. *Proceedings of the Physical Society. Section B*, 65(9):657–661, 1952.

[24] M. Sitti and R. Fearing. Synthetic gecko foot-hair micro/nano-structures as dry adhesives. *Journal of Adhesion Science and Technology*, 17(8):1055, 2003.

[25] O. Unver, M. Murphy, and M. Sitti. Geckobot and waalbot: Small-scale wall climbing robots. In *AIAA 5th Aviation, Technology, Integration, and Operations Conference*, 2005.

[26] O. Unver, A. Uneri, A. Aydemir, and M. Sitti. Geckobot: a gecko inspired climbing robot using elastomer adhesives. In *IEEE International Conference on Robotics and Automation*, pages 2329–2335, Orlando, FL, 2006.

[27] vortex. www.vortexhc.com, 2006.

[28] Z. Xu and P. Ma. A wall-climbing robot for labeling scale of oil tank's volume. *Robotica*, 20(2):203–207, 2002.

[29] H. Yao and H. Gao. Mechanics of robust and releasable adhesino in biology: Bottom-up designed hierarchical structures of gecko. *Journal of the mechanics and physics of solids*, 54:1120–1146, 2006.

[30] B. Yurdumakan, R. Raravikar, P. Ajayanb, and A. Dhinojwala. Syntheic gecko foot-hairs from multiwalled carbon nanotubes. *Chemical Communications*, 2005.

[31] Y. Zhao, T. Tong, L. Delzeit, A. Kashani, M. Meyyapan, and A. Majumdar. Interfacial energy and strength of multiwalled-carbon-nanotube-based dry adhesive. *Journal of Vacuum Science and Technology B*, 2006.

[32] J. Zhu, D. Sun, and S.K. Tso. Development of a tracked climbing robot. *Journal of Intelligent and Robotic Systems*, 35(4):427–444, 2002.